
Figures and figure supplements

Dynamic control of adipose tissue development and adult tissue homeostasis by platelet-derived growth factor receptor alpha

Sunhye Shin *et al*

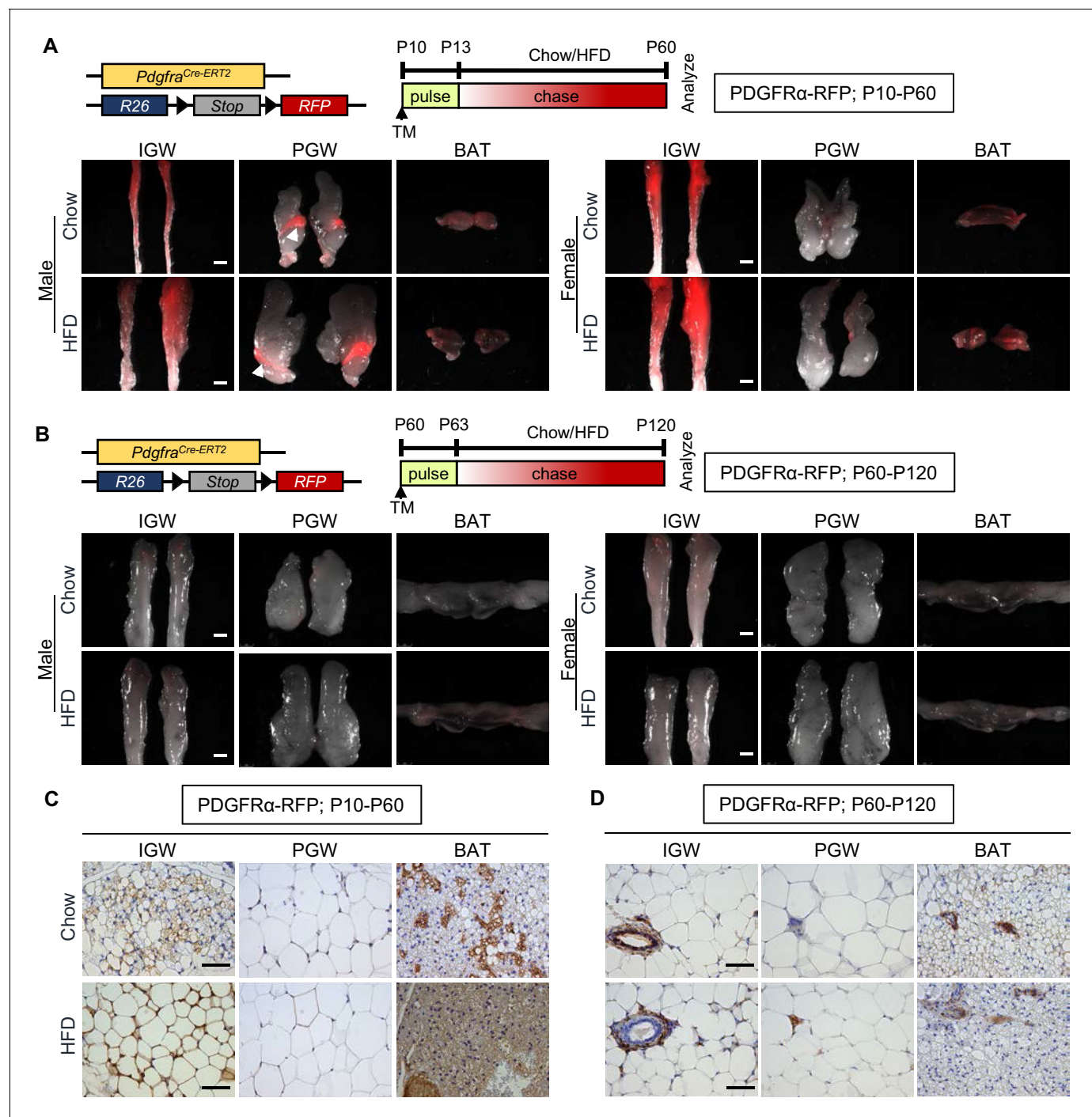


Figure 1. Developmental, but not adult, adipocytes derive from a PDGFR α + cell source. (A–B) *Pdgfra*^{Cre-ERT2}; *Rosa26*^{RFP} (PDGFR α -RFP) mice were administered tamoxifen (TM) (A) at postnatal day 10 (P10) and fed chow or HFD until P60 or (B) at P60 and fed chow or HFD until P120. IGW, PGW, and BATs were examined for direct RFP fluorescence either at (A) P60 or (B) P120 (chase). White arrowheads indicate the epididymis labeling. Scale = 100 μ m. (C–D) RFP staining of IGW, PGW, and BATs from above P10-P60 and P60-P120 mice using immunohistochemistry (IHC). Scale = 200 μ m.

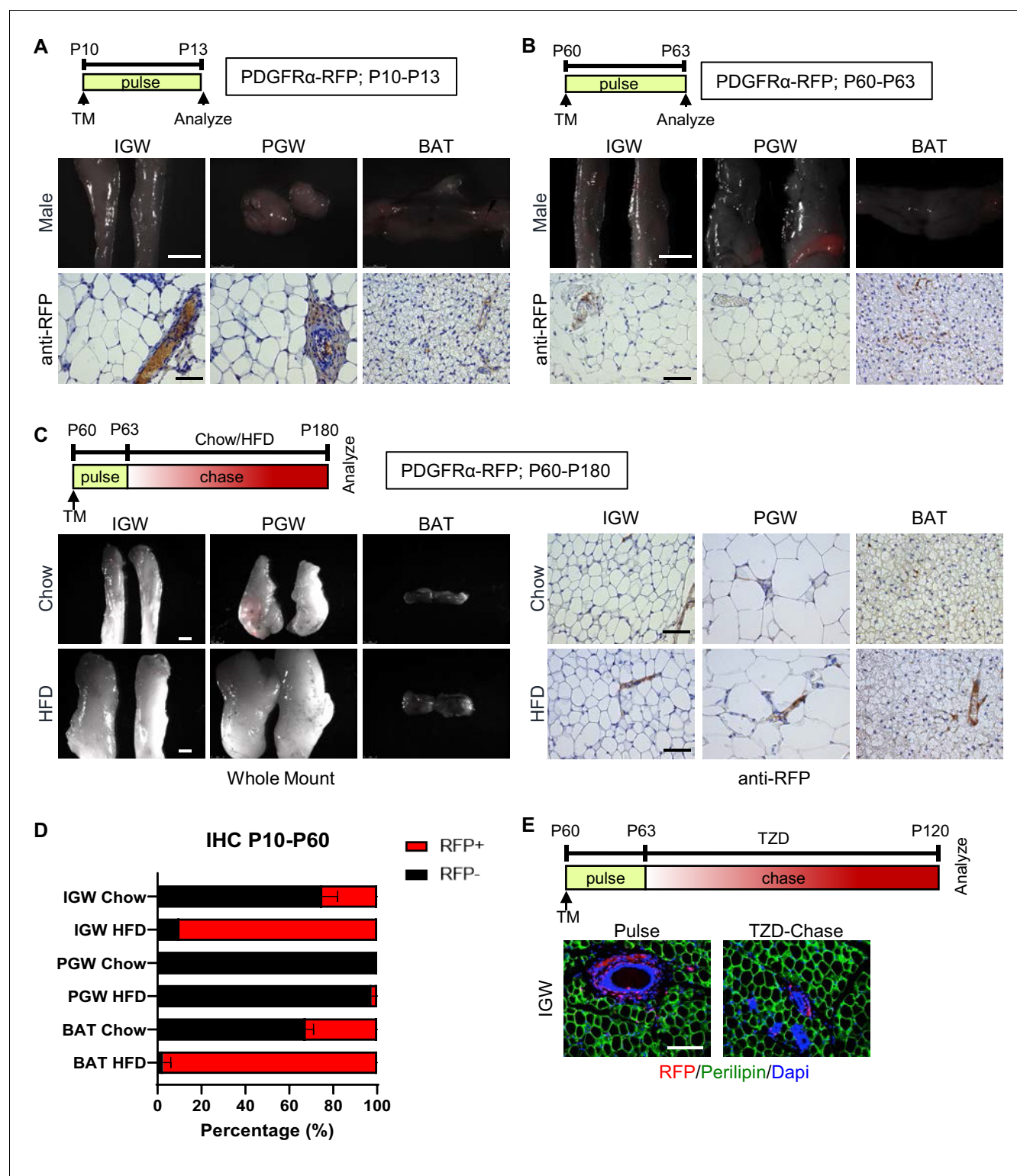


Figure 1—figure supplement 1. *Pdgfra*-dependent RFP expression at pulse, P60-P180, and P60-P120 TZD pulse-chase. (A–B) *Pdgfra*^{Cre-ERT2}; *Rosa26R*^{RFP} (PDGFR α -RFP) mice were administered TM (A) at postnatal day (P) 10 or (B) at P60. IGW, PGW, and BATs were examined for direct RFP fluorescence and RFP IHC staining after 3 days (pulse). Scale = 200 μ m. (C) PDGFR α -RFP mice were administered TM at P60 and fed chow or HFD until P180. IGW, PGW, and BATs were examined for direct RFP fluorescence and RFP IHC staining at P180 (chase). Scale = 100 μ m and 200 μ m. (D) Quantification of RFP+ adipocytes observed in randomly chosen 10 \times magnification fields from IGW, PGW, and BAT sections. (E) Confocal immunofluorescence image of a representative IGW section from animals treated with TZD. Sections were stained with anti-RFP (red) and anti-perilipin (green) antibodies and counterstained with DAPI (blue; nuclei). Scale = 200 μ m.

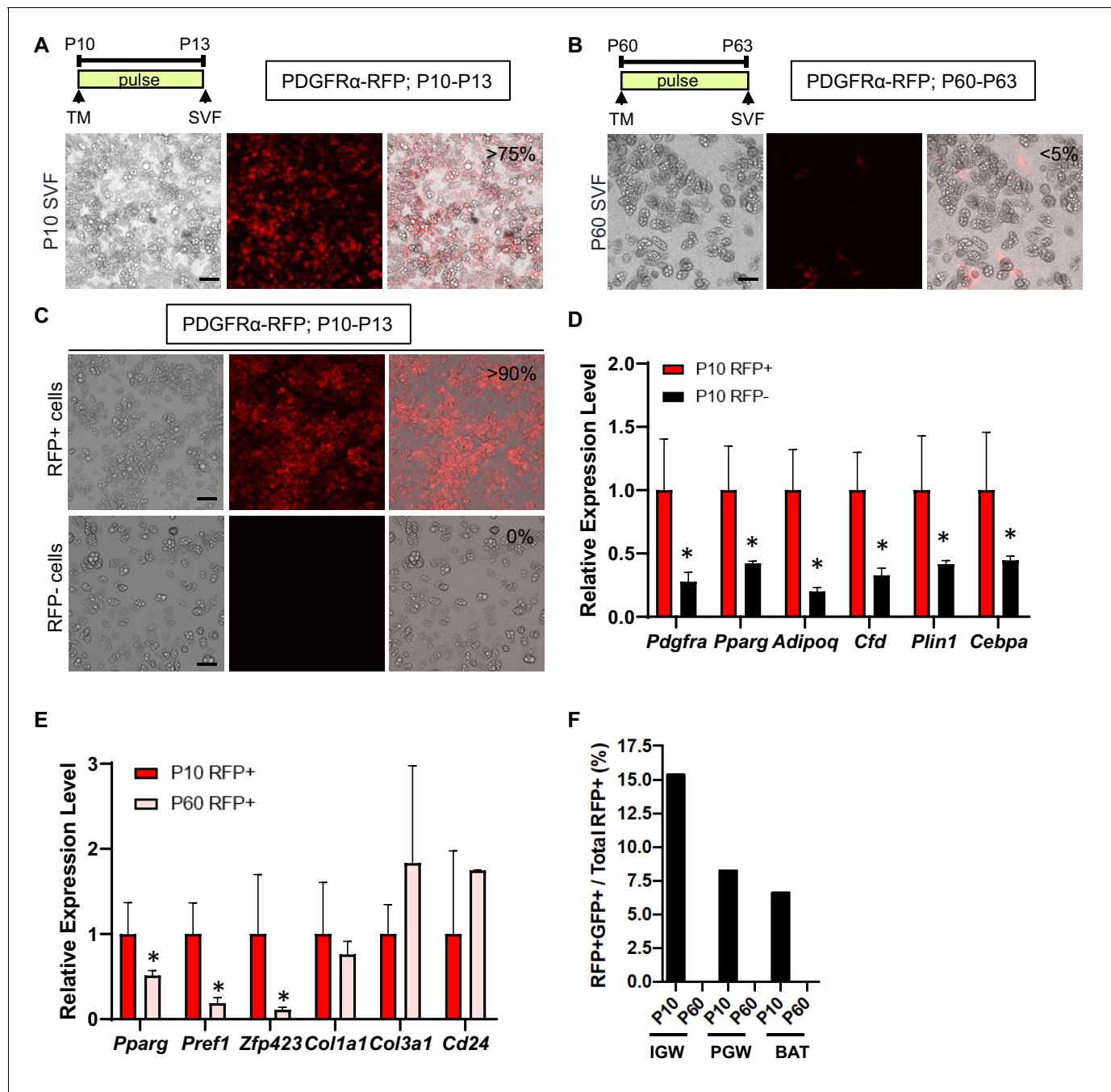


Figure 2. Developmental, but not adult, PDGFR α + cells are adipogenic. (A–B) *Pdgfra*^{Cre-ERT2}; *Rosa26*^{RFP} (PDGFR α -RFP) male mice were administered TM at P10 (A) or P60 (B). Stromal vascular fraction of cells (SVF) were isolated from IGW of the mice after 3 days and cultured. The numbers indicate the percentage of the RFP+ labeled adipocytes. Scale = 100 μ m. (C) TM-induced PDGFR α -RFP male mice either at P10 or P60 were fed chow or HFD until P120. SVF were isolated from IGW of the mice at P120, cultured, and examined for direct RFP fluorescence. Scale = 100 μ m. (D) The real-time q-PCR analysis of adipogenic markers from cells described in C. * $p < 0.05$ P10 RFP- compared to P10 RFP+ cells. (E) Gene expression levels of P10 and P60 RFP+ cells in SVF isolated from pooled IGW ($n = 10$). * $p < 0.05$ P60 RFP+ compared to P10 RFP+ cells. Data are expressed as mean \pm SEM. (F) *Pparg*^{TA}-H2BGFP; PDGFR α -RFP male mice were administered TM at P10 or P60. SVF were isolated from the pooled IGW, PGW, and BAT depots ($n = 8$) after 3 days and sorted using RFP signal. GFP+RFP+ cells were quantified.

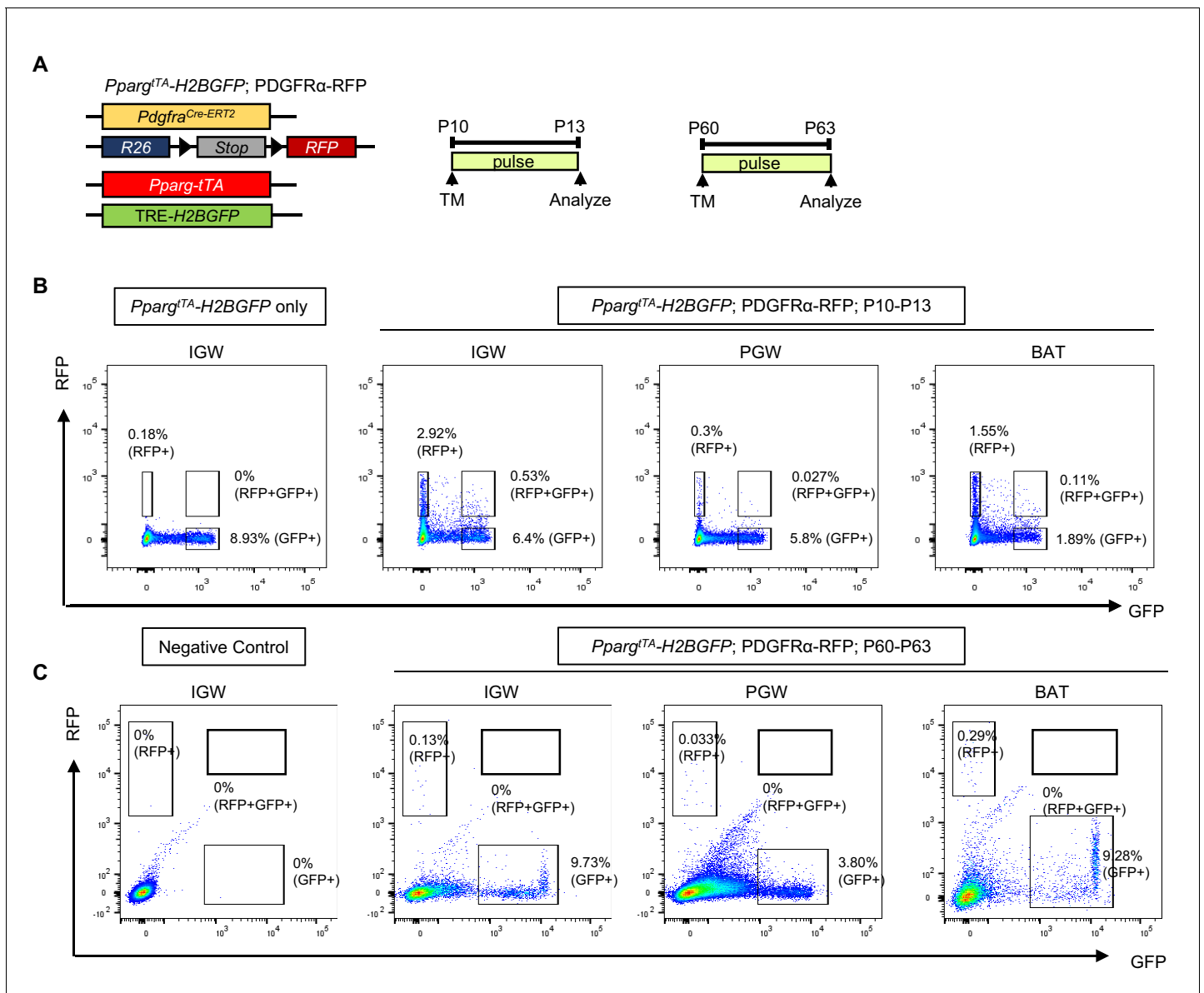


Figure 2—figure supplement 1. Developmental, but not adult, PDGFR α ⁺ cells overlap with PPAR γ ⁺ cells. (A) Schematic of *Pparg*^{tTA-H2BGFP}; PDGFR α -RFP male mice breeding. Mice were administered TM at P10 or P60. SVF were isolated after 3 days. GFP+RFP+ cells were quantified in IGW, PGW, and BAT. (B) The flow analysis of P10 labeled PDGFR α -RFP cells overlapping with *Pparg*^{tTA} labeled GFP+ cells. The numbers indicate the percentage of total SVF in IGW, PGW, and BAT (pooled SVF from n = 10 mice). (C) The flow analysis of P60 labeled PDGFR α -RFP cells overlapping with *Pparg*^{tTA} labeled GFP+ cells. The numbers indicate the percentage of total SVF in IGW, PGW, and BAT (pooled SVF from n = 8 mice).

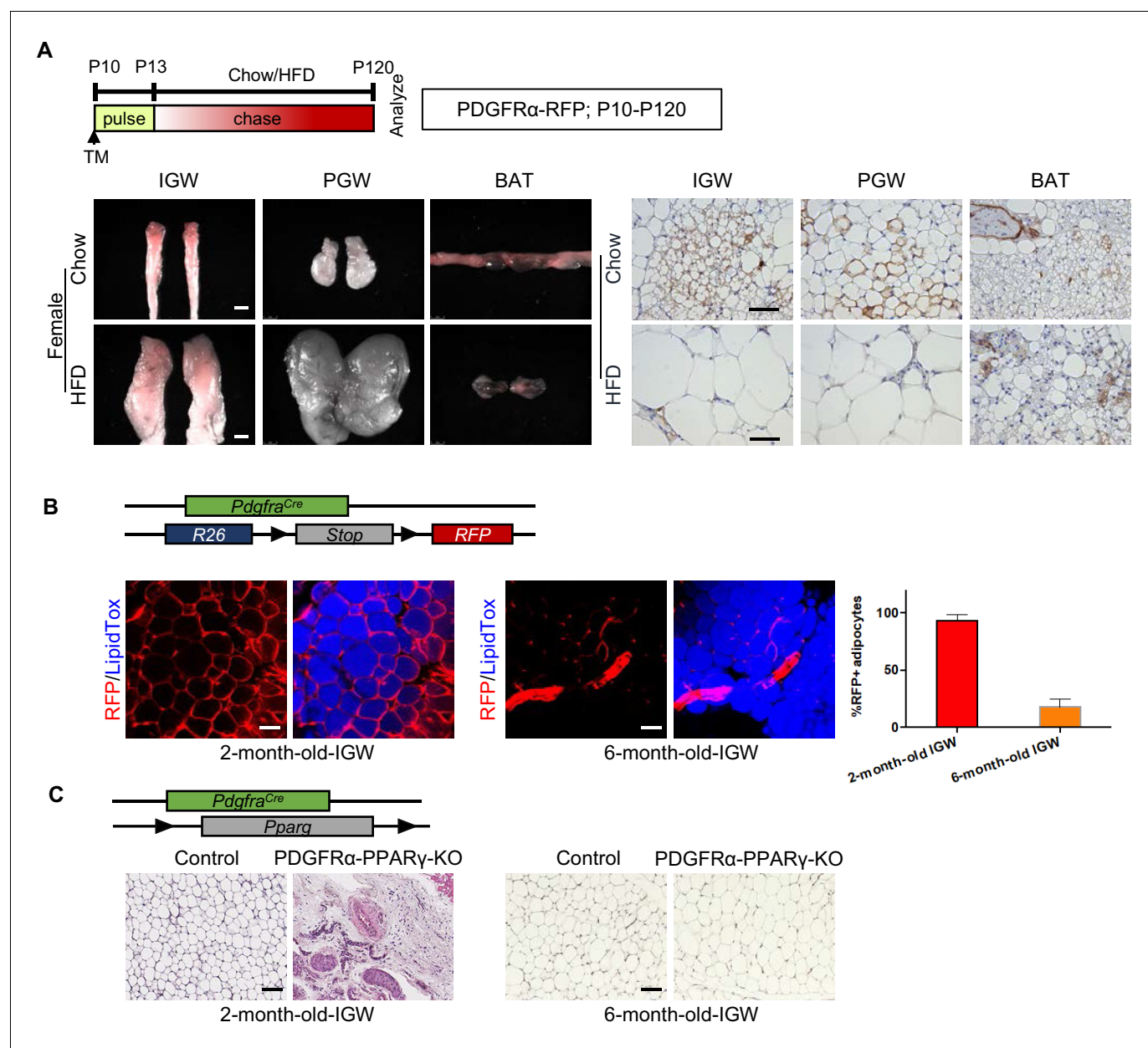


Figure 3. Developmental PDGFR α + cells contribute to postnatal but not adult WAT development. (A) *Pdgfra*^{Cre-ERT2}; *Rosa26*^{RFP} (PDGFR α -RFP) mice were administered TM (A) at postnatal day (P) 10 and fed chow or HFD until P120. IGW, PGW, and BATs were examined for direct RFP fluorescence and RFP IHC staining. Scale = 100 μ m and 200 μ m. (B) A 2- and 6-month-old PDGFR α -RFP mice were analyzed. IGWs were examined for direct RFP fluorescence and stained with LipidTox (blue). The quantifications for numbers of RFP+ adipocytes were calculated. Scale = 100 μ m. (C) A 2- and 6-month-old control and *Pdgfra*^{Cre}; *Pparg*^{fl/fl} (PDGFR α -PPAR γ -KO) mice were analyzed. IGWs were examined using hematoxylin and eosin (H&E) staining. Scale = 100 μ m.

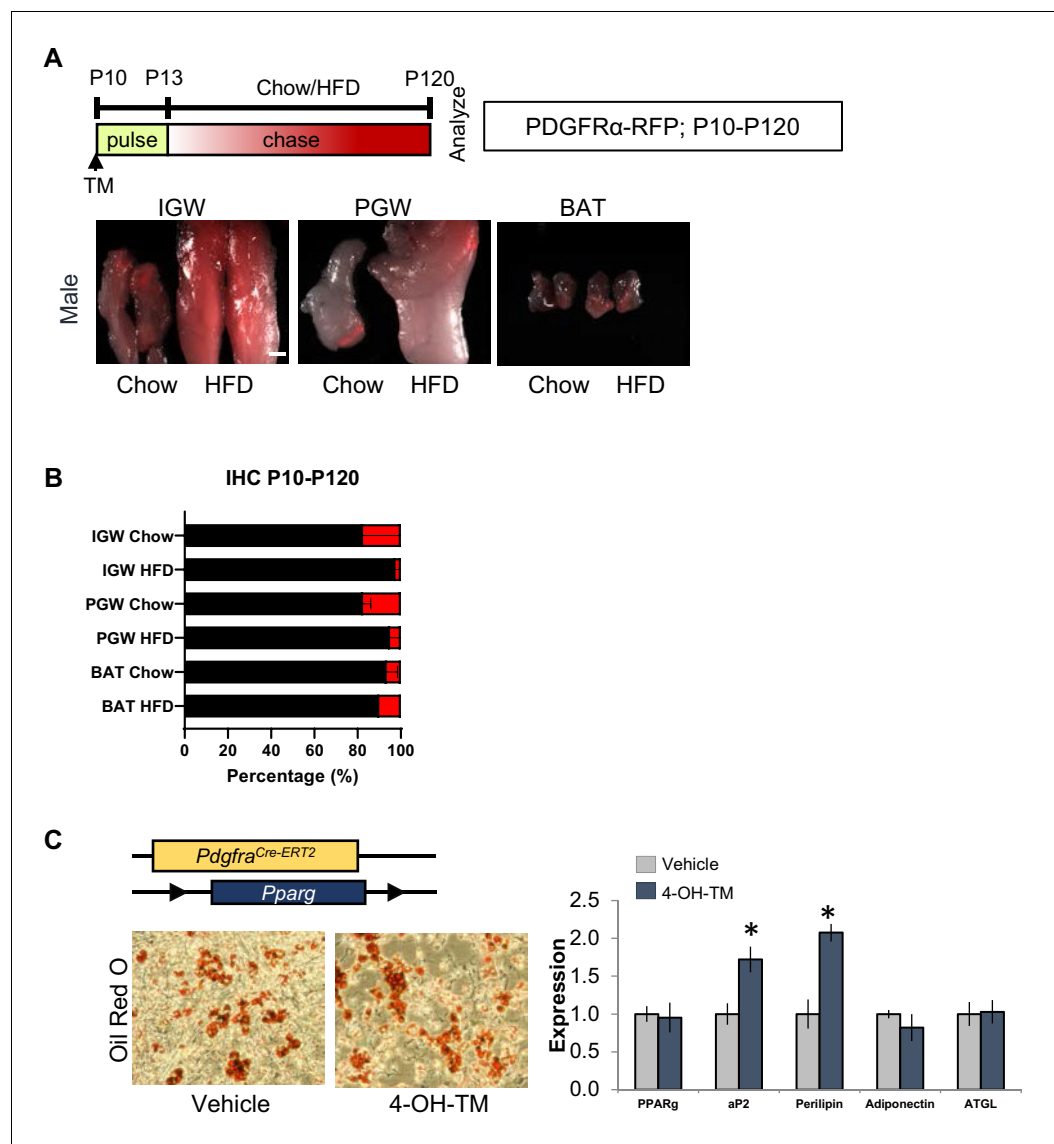


Figure 3—figure supplement 1. P10 PDGFR α ⁺ cells contribute to postnatal but not adult WAT development. (A) *Pdgfra*^{Cre-ERT2}; *Rosa26R*^{RFP} (PDGFR α -RFP) mice were administered TM (A) at postnatal day (P) 10 and fed chow or HFD until P120. IGW, PGW, and BATs were examined for direct RFP fluorescence. Scale = 100 μ m. (B) Quantification of RFP⁺ adipocytes observed in randomly chosen 10X magnification fields from IGW, PGW, and BAT sections. (C) Oil Red O staining and gene expression analysis of SVF adipogenesis from IGW of *Pdgfra*^{Cre-ERT2}; *Pparg*^{fl/fl} male mice at P60, either veh or 4-OH-tamoxifen (4-OH-TM) treated. *p<0.05 TM compared to Veh cells. Data are expressed as mean \pm SEM.

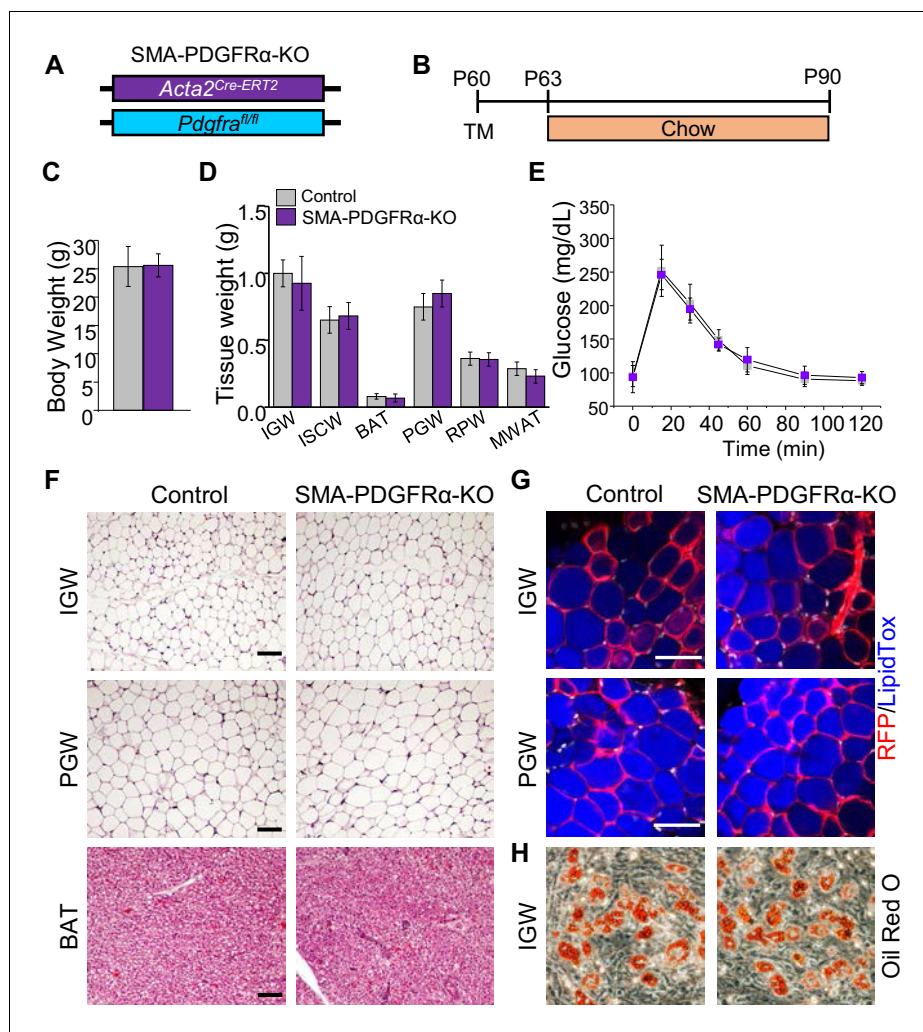


Figure 4. Deleting *Pdgfra* in adult SMA+ APCs is dispensable for adult white adipogenesis. (A–B) *Acta2*^{Cre-ERT2}, *Pdgfra*^{fl/fl} male control and mutant (SMA-PDGFR α -KO) mice were administered TM at P60 and analyzed at P90. (C) Body weight of control and SMA-PDGFR α -KO mice at P90. Data are expressed as mean \pm SEM. (D) Adipose tissue weights. Data are expressed as mean \pm SEM. (E) Blood glucose level during glucose tolerance test. Data are expressed as mean \pm SEM. (F) Hematoxylin and eosin (H&E) staining of IGW, PGW, and BAT. Scale = 100 μ m. (G) IGW and PGW were analyzed for direct RFP fluorescence and stained with LipidTox. Scale = 200 μ m. (H) Oil Red O staining of SVF adipogenesis from IGW of control and SMA-PDGFR α -KO male mice at P90.

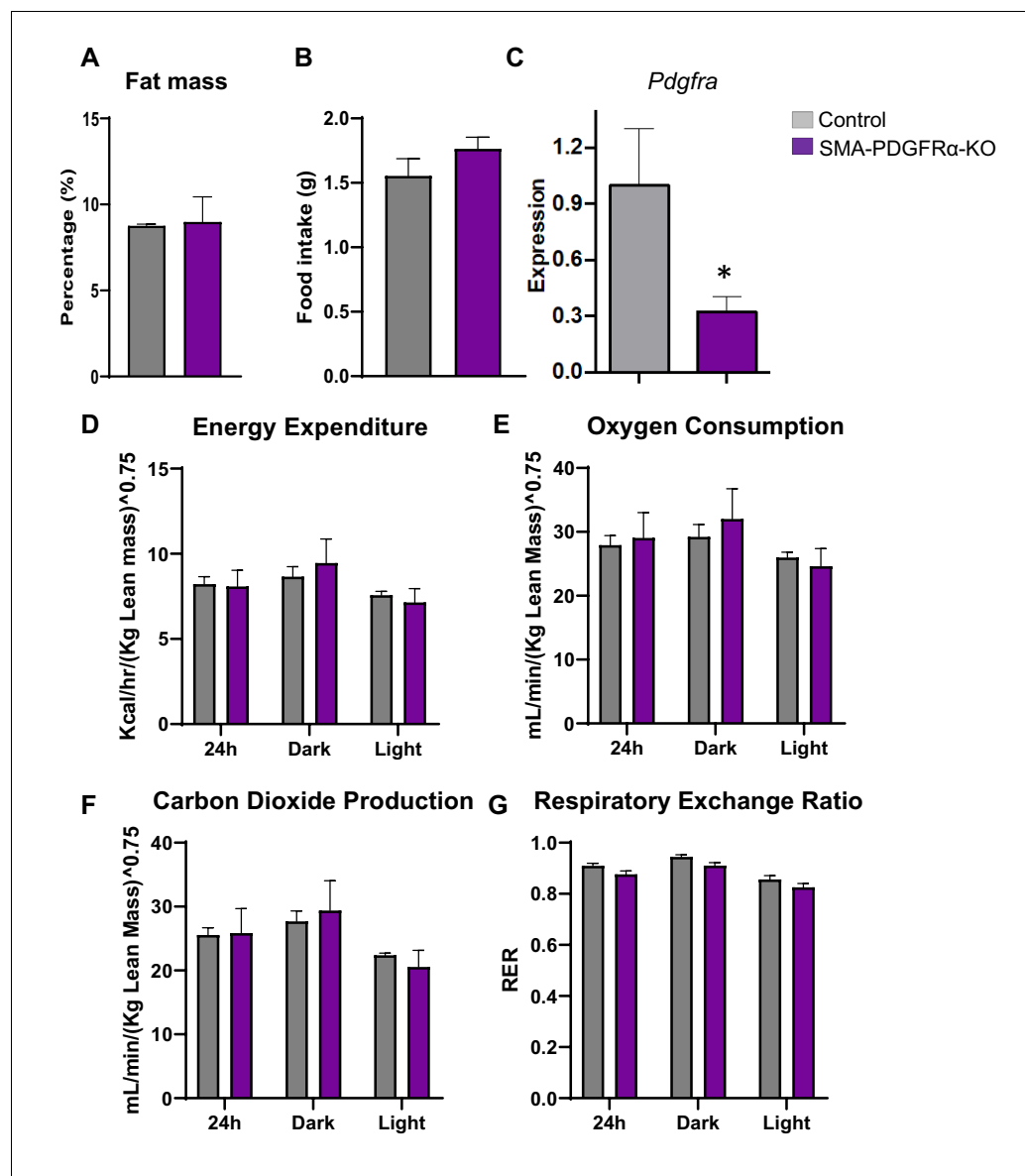


Figure 4—figure supplement 1. SMA-PDGFR α -KO mice do not display abnormal energy expenditure. (A) Body fat mass of *Acta2^{Cre-ERT2}; Pdgfra^{fl/fl}* male control and SMA-PDGFR α -KO mice at P90. Data are expressed as mean \pm SEM. (B) Food intake of control and SMA-PDGFR α -KO mice. Data are expressed as mean \pm SEM. (C) A real-time q-PCR analysis of the *Pdgfra* level in BAT of control and SMA-PDGFR α -KO mice. * $p < 0.05$ SMA-PDGFR α -KO mice compared to control mice. Data are expressed as mean \pm SEM. (D) Energy expenditure of control and SMA-PDGFR α -KO mice. Data are expressed as mean \pm SEM. (E) Oxygen consumption of control and SMA-PDGFR α -KO mice. Data are expressed as mean \pm SEM. (F) Carbon dioxide production of control and SMA-PDGFR α -KO mice. Data are expressed as mean \pm SEM. (G) Respiratory exchange ratio of control and SMA-PDGFR α -KO mice. Data are expressed as mean \pm SEM.

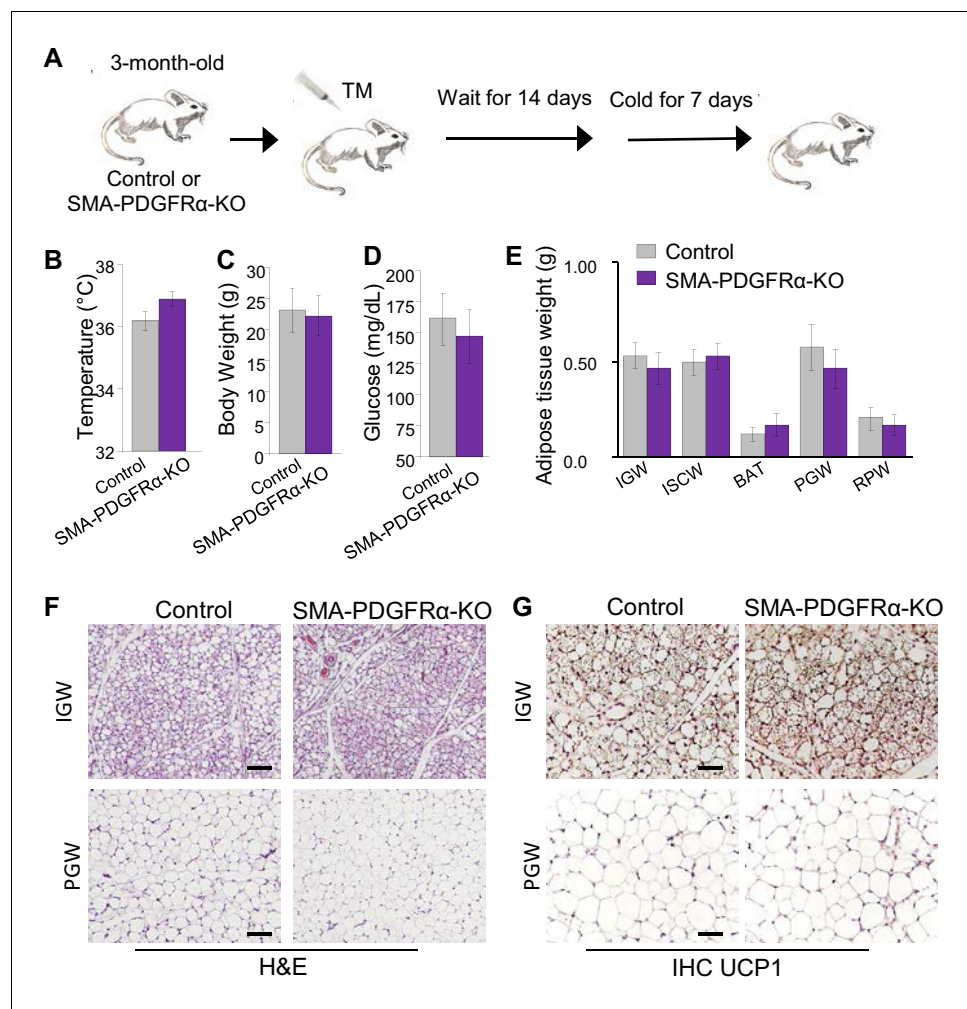


Figure 5. Deleting *Pdgfra* in adult SMA+ APCs is dispensable for cold-induced beige adipogenesis. (A) A 3-month-old *Acta2^{Cre-ERT2}; Pdgfra^{fl/fl}* male control and SMA-PDGFR α -KO mice were administered TM. After 14 days of TM washout, the mice were cold-exposed for 7 days. (B) Rectal temperature after cold exposure. Data are expressed as mean \pm SEM. (C) Body weight after cold exposure. Data are expressed as mean \pm SEM. (D) Blood glucose after cold exposure. Data are expressed as mean \pm SEM. (E) Adipose tissue weight. Data are expressed as mean \pm SEM. (F) Hematoxylin and eosin (H&E) staining of IGW and PGW. Scale = 100 μ m. (G) UCP1 staining of IGW and PGW using immunohistochemistry (IHC). Scale = 100 μ m.

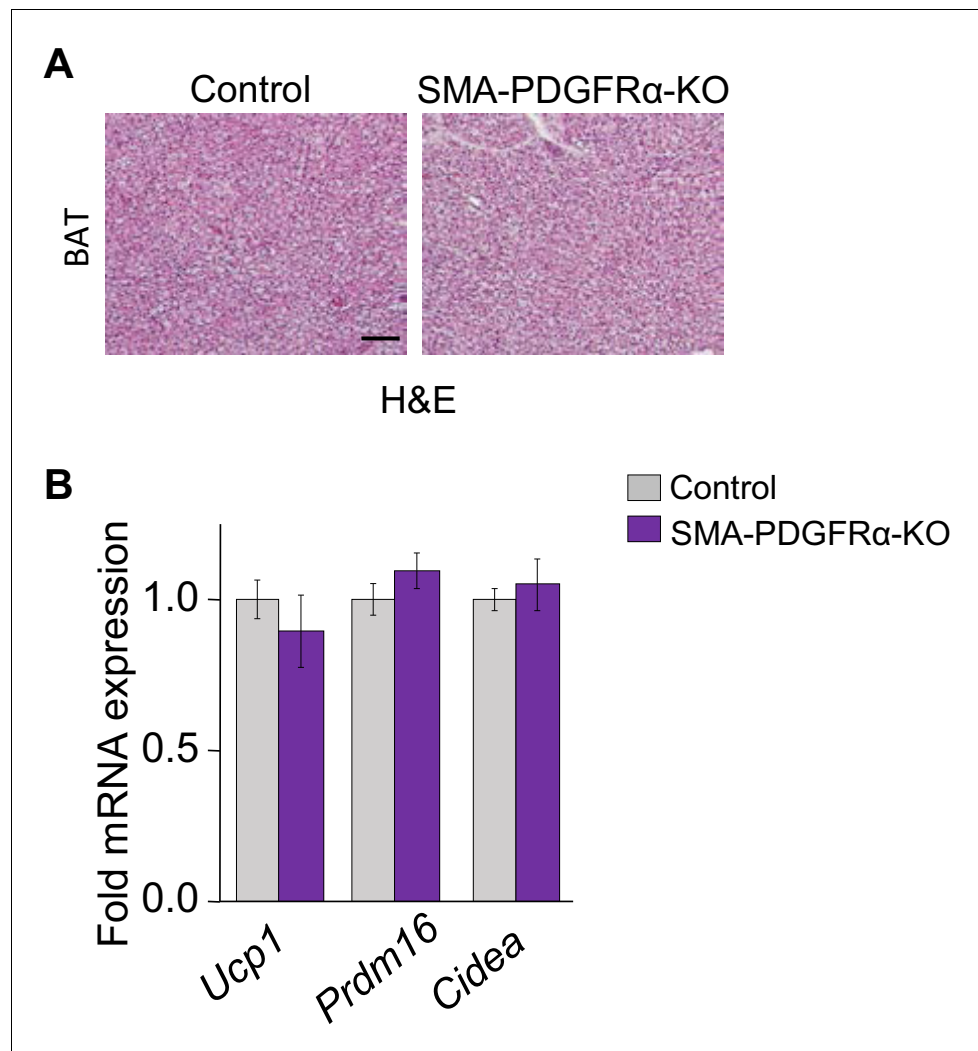


Figure 5—figure supplement 1. Deleting *Pdgfra* in adult SMA+ APCs is dispensable for cold-induced beige adipogenesis. (A) A 3-month-old *Acta2*^{Cre-ERT2}; *Pdgfra*^{fl/fl} male control and SMA-PDGFR α -KO mice were administered TM. After 14 days of TM washout, the mice were cold-exposed for 7 days. H&E staining of BAT. Scale = 100 μ m. (B) Thermogenic gene expression levels in control and SMA-PDGFR α -KO IGW. Data are expressed as mean \pm SEM.

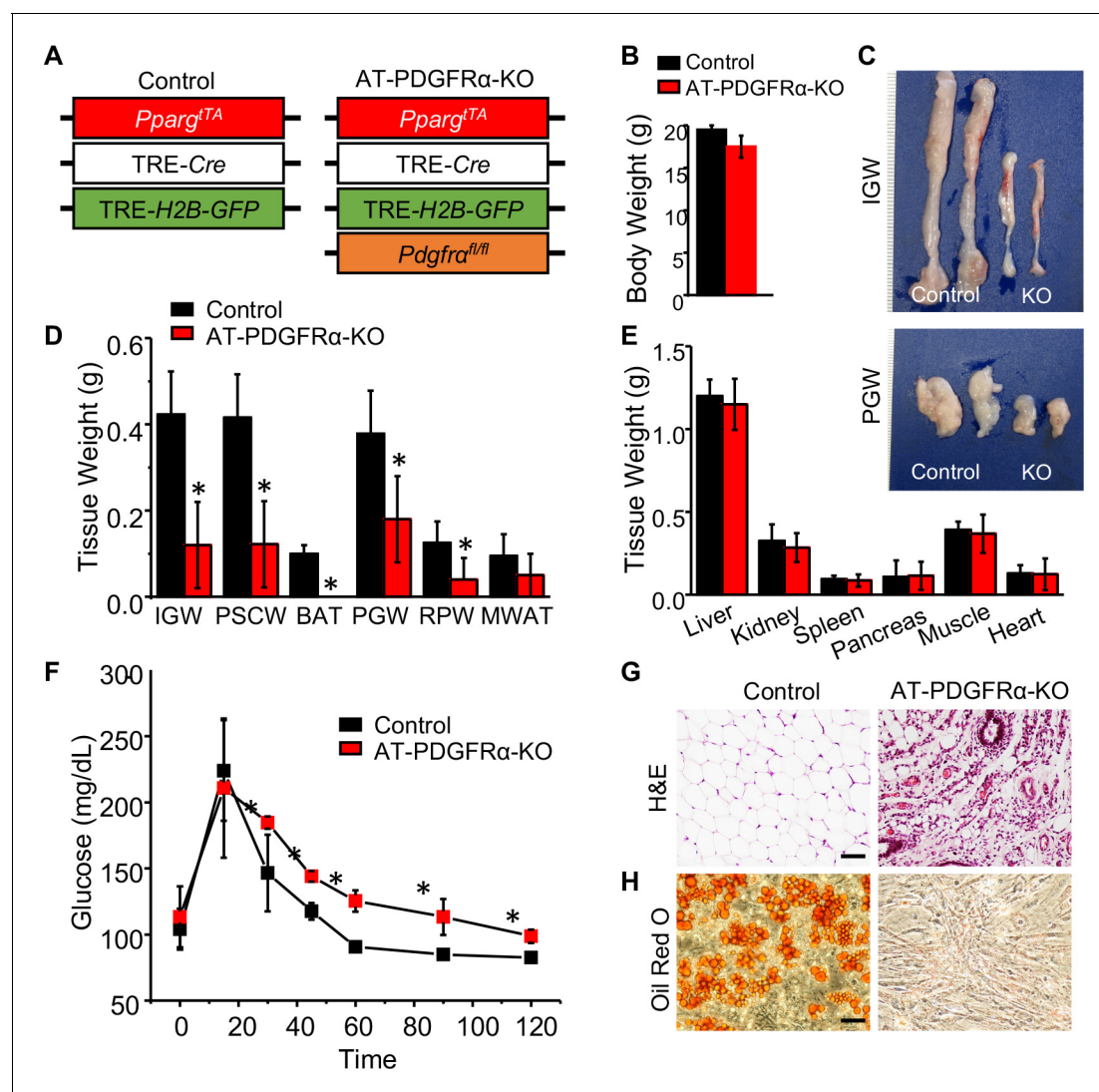


Figure 6. PDGFR α in developmental APCs is essential for adipose tissue development. (A) A 2-month-old *Pparg*^{fl/fl}; TRE-Cre; TRE-H2B-GFP; *Pdgfra*^{fl/fl} male control and AT-PDGFR α -KO mice were analyzed. (B) Body weight. Data are expressed as mean \pm SEM. (C) IGW and PGW tissue. (D) Adipose tissue weight. *p<0.05 AT-PDGFR α compared to AT-Con mice. Data are expressed as mean \pm SEM. (E) Other tissue weight. Data are expressed as mean \pm SEM. (F) Blood glucose level during glucose tolerance test. *p<0.05 AT-PDGFR α -KO compared to control mice. Data are expressed as mean \pm SEM. (G) Hematoxylin and eosin (H&E) staining of IGW. Scale = 100 μ m. (H) Oil Red O staining of SVF isolated from IGW of control and AT-PDGFR α -KO mice.

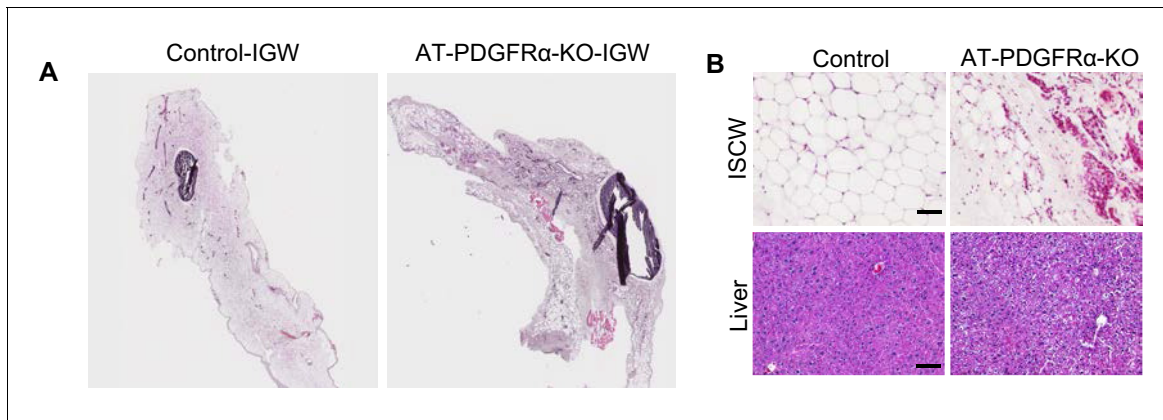


Figure 6—figure supplement 1. PDGFR α in developmental APCs is essential for adipose tissue development. (A) IGW tissues of 2-month-old *Pparg*^{tTA}; TRE-Cre; TRE-H2B-GFP; *Pdgfra*^{fl/fl} male control and AT-PDGFR α -KO mice. (B) Hematoxylin and eosin (H&E) staining of ISCW and liver of control and AT-PDGFR α -KO mice. Scale = 100 μ m.

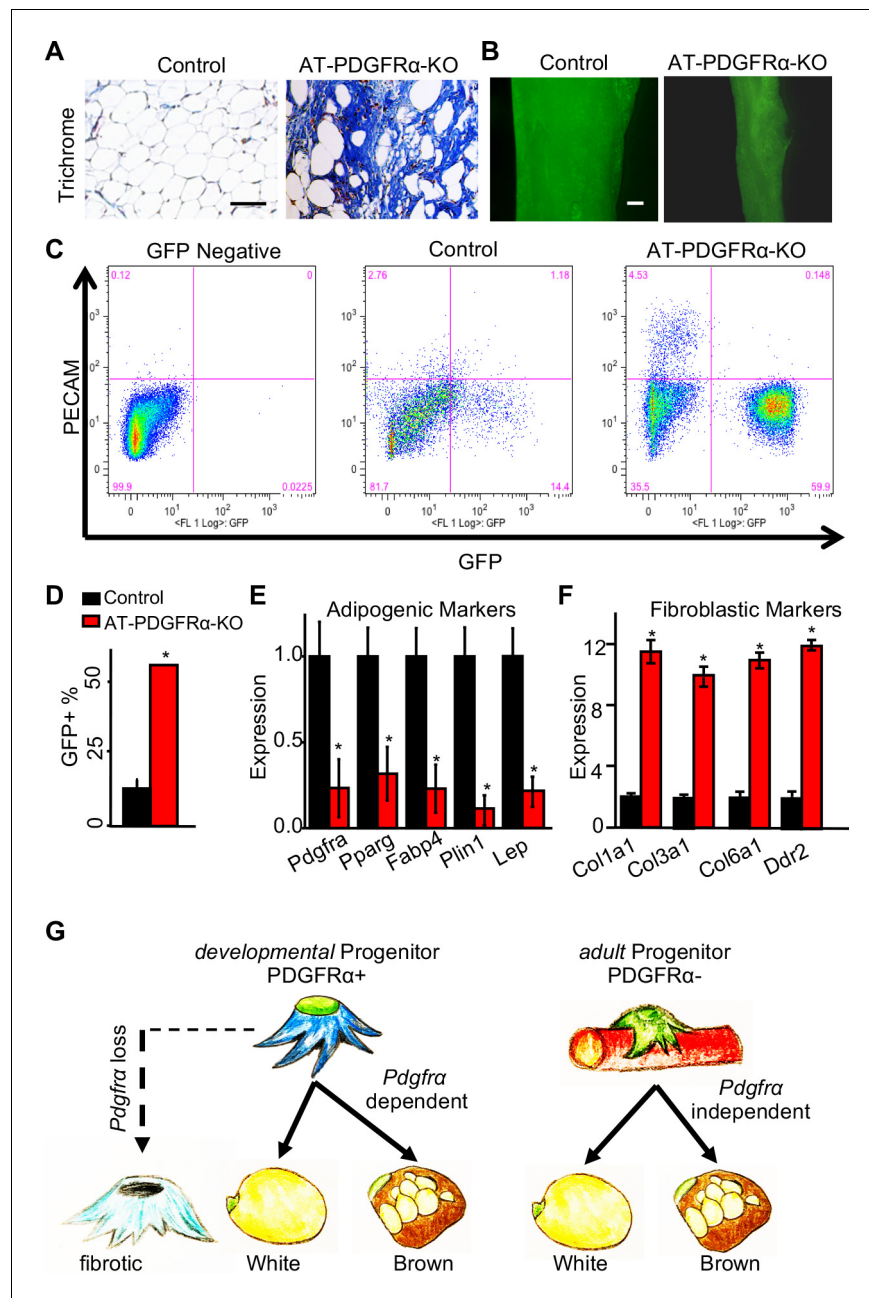


Figure 7. PDGFR α regulates adipose tissue development through lineage control. (A) A 2-month-old *Pparg*^{TA}; TRE-Cre; TRE-H2B-GFP; *Pdgfra*^{fl/fl} male control and AT-PDGFR α -KO mice were analyzed. Trichrome staining of IGW. Scale = 200 μ m. (B) Direct GFP fluorescence of IGW. Scale = 100 μ m. (C) Flow cytometry profiles of SVF isolated from IGW. (D) Quantification of GFP+ adipose progenitor cell number. Data are expressed as mean \pm SEM. (E) Adipogenic marker gene expression levels in GFP+ cells of SVF isolated from IGW. Data are expressed as mean \pm SEM. (F) Fibrotic marker gene expression levels in GFP+ cells of SVF isolated from IGW. Data are expressed as mean \pm SEM. * p <0.05 AT-PDGFR α -KO compared to control mice in D-F. (G) Working model for PDGFR α in developmental and adult progenitors. Developmental progenitors are marked by PDGFR α and adipogenesis is dependent on PDGFR α . In the absence of PDGFR α , developmental progenitors switch the lineage to fibrotic. Adult progenitors for WAT homeostasis are not marked by PDGFR α and adipogenesis during WAT homeostasis is largely PDGFR α independent.

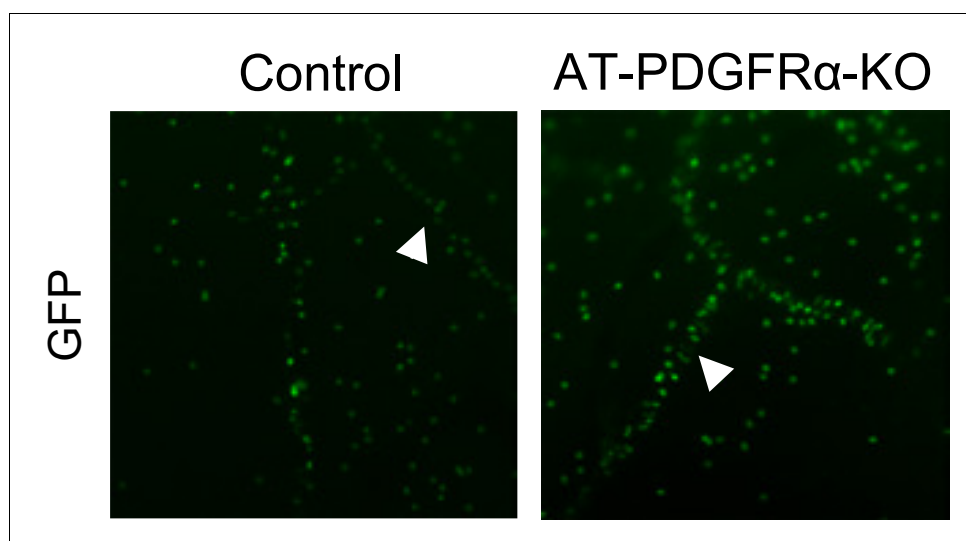


Figure 7—figure supplement 1. *Pdgfra* deletion in developmental APCs. IGW tissues of P60 *Pparg*^{tTA}; TRE-Cre; TRE-H2B-GFP; *Pdgfra*^{fl/fl} male control and AT-PDGFR α -KO mice. White arrowheads indicate the GFP+ progenitors align on the vasculature.